Progress In Electromagnetics Research Letters, Vol. 105, 63–69, 2022

Finsler Metric Method for Ship Detection in SAR Image

Huafei Zhao and Meng Yang[1*]

Abstract—In this article, we focus on metric space in Finsler geometry and propose a method of ship detection in synthetic aperture radar (SAR) amplitude image based on Finsler information geometry. This provides deep unified perspectives of Finsler geometric application. The proposed method consists of three stages: The Weibull manifold model is used to represent the statistical information of intensity SAR images; then the Finsler metric is constructed to realize the distance measurement between probability distributions in Weibull manifold space; finally, Finsler metric space is used to achieve saliency representation and detection of ships. Theoretical analysis and comprehensive experimental results demonstrate the robustness and effectiveness of the proposed approach using typical real SAR images.

1. INTRODUCTION

The aim of a synthetic aperture radar (SAR) is to form an image which represents the radar reflectivity of the scene being imaged. Modern SAR sensors can generate large amounts of data in a short period of time, and there is an obvious need for automatic detection of targets of interest. Automatic ship target detection based on SAR image is an important part of marine remote sensing application [1].

Ship detection algorithms can be mainly divided into traditional algorithms and deep learning based algorithms. Most traditional algorithms are based on modelling the background statistically and then finding individual pixels or small groups of neighbouring pixels whose brightness values are statistically unusual. Among these algorithms, constant false alarm rate (CFAR) technique is widely used in SAR targets detection [2]. On the one hand, designing a CFAR detector involves solving the complex equation for the adaptive threshold in terms of the specified false alarm rate (FAR) and the estimated parameters of the probability density function. On the other hand, because of the fluctuant and complex background in SAR, CFAR detection technology may suffer from performance deterioration due to the changes in ship imaging quality and the influence of complex and unpredictable surroundings [3]. From the deep learning perspective, a large number of high quality samples are required in many algorithms [4]. In some applications, observation on big samples lacks, and cooperated standard detection research is deficient. Experience has shown that no one algorithm or even combination of algorithms will do this perfectly. Now no detector is generally accepted, and care needs to be taken with the type of SAR imagery which it is applied [5].

This letter aims to investigate the metric space and related topics of Finsler geometry, and some use cases of these geometric structures in ship detection of SAR image. According to the common methods of information geometry modeling [6], one solution is to apply Finsler geometric analysis method to investigate the properties of families of probability distributions. It is devoted to the study of geometric structures modeled on parameter spaces and establishes the local structure of Finsler manifolds that carry such a structure.

Received 27 March 2022, Accepted 14 July 2022, Scheduled 24 July 2022
* Corresponding author: Meng Yang (yangmeng@hdu.edu.cn).
The authors are with the Hangzhou Dianzi University, Hangzhou, China.

The innovation of this article lies in: It puts forward a feasible way for applying Finsler geometric theory in ship detection of SAR images; it also provides a feasible framework for further in-depth investigation of Finsler information geometry theory and applications in SAR image analysis.

2. PROPOSED METHODS

Information geometry has emerged from investigating the geometrical structure of a family of probability distributions. It has been applied successfully to various areas. This letter offers a new entry point for application of information geometry from a more general point of view using Finsler geometry.

2.1. Finsler Metric

The geometrical data in Finsler geometry consists of a smoothly varying family of Minkowski norms, rather than a family of inner products. This family of Minkowski norms is known as Finsler structure. Let $\mathcal{M}$ be an n-dimensional smooth manifold, $T\mathcal{M}$ be the tangent bundle, and $F : TM \to [0, +\infty)$ be a function on the tangent bundle $T\mathcal{M}$. F is called a Finsler metric in $\mathcal{M}$ if it satisfies the following conditions [7]:
(1) $F(x, \lambda y) = \lambda F(x, y)$, $\forall \lambda > 0$;
(2) $F(x, y)$ is a $\mathbb{C}^\infty$ function on $TM\backslash\{0\}$;
(3) $\forall y \neq 0$, $g_{ij}(x, y) = \frac{1}{2}\frac{\partial^2 F^2}{\partial y^i \partial y^j}(x, y) = \frac{1}{2}\left(F^2\right)_{y^i y^j}$ is positively definite.
A differential manifold $\mathcal{M}$ equipped with a Finsler metric F is called a Finsler space or Finsler manifold.

2.2. Weibull Manifold

Speckle is a fundamental property of SAR imagery. It is only noise-like rather than an actual noise process. Its cause lies in the scattering of coherent radar waves from rough ocean surface. Without loss of generality, we adopt the well-known two-parameter Weibull distribution for modeling sea clutter in SAR images. In general, we say that Z is a Weibull random variable on the interval $[0, +\infty)$ if the probability density function of Z is given by [8]

$$W\left(z\,|\alpha, \beta\,\right) = \frac{\alpha}{\beta}\left(\frac{z}{\beta}\right)^{\alpha-1} \exp\left[-\left(\frac{z}{\beta}\right)^{\alpha}\right] \tag{1}$$

where $\alpha > 0$ and $\beta > 0$ denote the shape and scale parameters, respectively. Hence, we define a matrix $[a_{ij}(x)]$,

$$\left[a_{ij}\left(x\right)\right] = \begin{bmatrix} \dfrac{\beta^{2\tau}}{\alpha^2} & \dfrac{\gamma-1}{\alpha} \\ \dfrac{\gamma-1}{\alpha} & \dfrac{(\gamma-1)^2+\pi^2/6}{\beta^{2\tau}} \end{bmatrix} \tag{2}$$

where $x = (\alpha, \beta)$, γ is the Euler's constant (approximated by 0.5772), and $[a_{ij}(x)]$ is a symmetric, smooth, positively definite matrix, and

$$\tau = 25\beta\sqrt{\Gamma\left[(\alpha+2)/\alpha\right] - \Gamma^2\left[(\alpha+1)/\alpha\right]} \tag{3}$$

where Γ denotes the Gamma function. Thus, a Finsler metric F is defined by

$$F\left(x, y\right) = \frac{\left(\sqrt{|y|^2 + \langle x, y\rangle^2 - |x|^2|y|^2} + \langle x, y\rangle\right)^2}{\left(1 - |x|^2\right)^2\sqrt{|y|^2 + \langle x, y\rangle^2 - |x|^2|y|^2}} \tag{4}$$

where $y = (y^i)$, $y \in T_x\mathcal{M}$, $x = (x^i) \in \mathcal{M}$, and $|y|^2 = \langle y, y\rangle = \sqrt{a_{ij}y^i y^j}$.

2.3. Detection Algorithm for Ships

In the following, we present the main steps of the detection algorithm:
(1) The simple linear iterative clustering (SLIC) method [9] is applied to superpixel segmentation of SAR images;
(2) The shape and scale parameters (α, β) are estimated by using maximum likelihood estimation (MLE) technique based on each superpixel;
(3) The Finsler metric F of each superpixel in the SAR image is calculated with respect to the parameters (α, β);
(4) The final detection is realized by using the maximum interclass variance method [10].

3. EXPERIMENTAL RESULTS AND ANALYSIS

To verify the effectiveness of the proposed approach, the performance assessment of the method has been carried out over two SAR images, as shown in Figs. 1(a) and (b). To reduce the computational complexity, the proposed method works on superpixel-based data rather than pixel-based data. By using the method of SLIC, we obtain the results of image segmentation given by the experimental parameter: the superpixel size 10×10 pixels. As shown in Figs. 2(a) and (b), the experimental results demonstrate the effectiveness of SLIC for segmentation of SAR images.

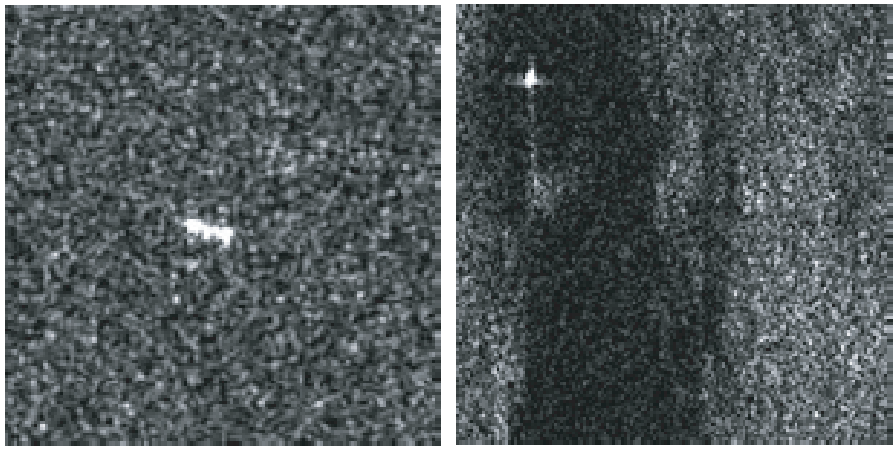

(a) (b)

Figure 1. SAR images of the sea surface. (a) SAR image. (b) SAR image.

Based on superpixels and the assumptions, the shape and scale parameters (α, β) are estimated by MLE technique. Let $y^1 = \alpha$, $y^2 = \beta$ and $\tau = 6$. The Finsler metrics F of superpixels in the SAR images are calculated with respect to the parameters (α, β). Figs. 3(a) and (b) show the Finsler metrics for superpixels that showed target-background differences in the high contrast.

The final detection results are obtained by using the maximum interclass variance method. As shown in Figs. 4(a) and (b), the proposed method is able to provide desirable detection results for SAR images.

To verify the advantage of the proposed approach, the performance of the double-parameter CFAR and the superpixel-level CFAR detectors under Weibull background are studied. The experimental parameters are set as follows: the guard-band of 10×10 pixels, the background-band of 25×25 pixels, and the constant false alarm rate 10^{-7}. Here, the double-parameter CFAR detector utilizes the classic rectangular guard/backgroud band topology, while the superpixel-level CFAR detector utilizes superpixels to define the guard and background bands. Fig. 5 and Fig. 6 show the detection results obtained by using the double-parameter CFAR and the superpixel-level CFAR [11] detectors under Weibull background, which cause false alarm even though it works at a low false alarm rate. Actually,

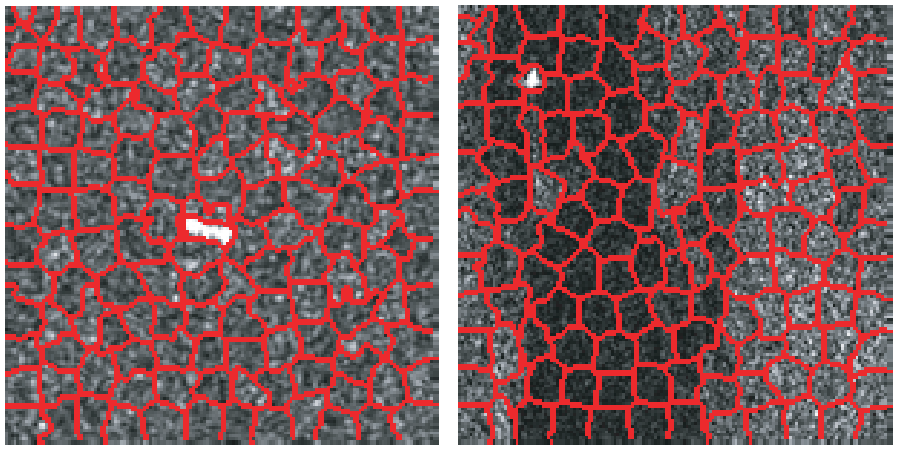

(a) (b)

Figure 2. Class segmentation with superpixel neighborhoods. (a) Fig. 1(a). (b) Fig. 1(b).

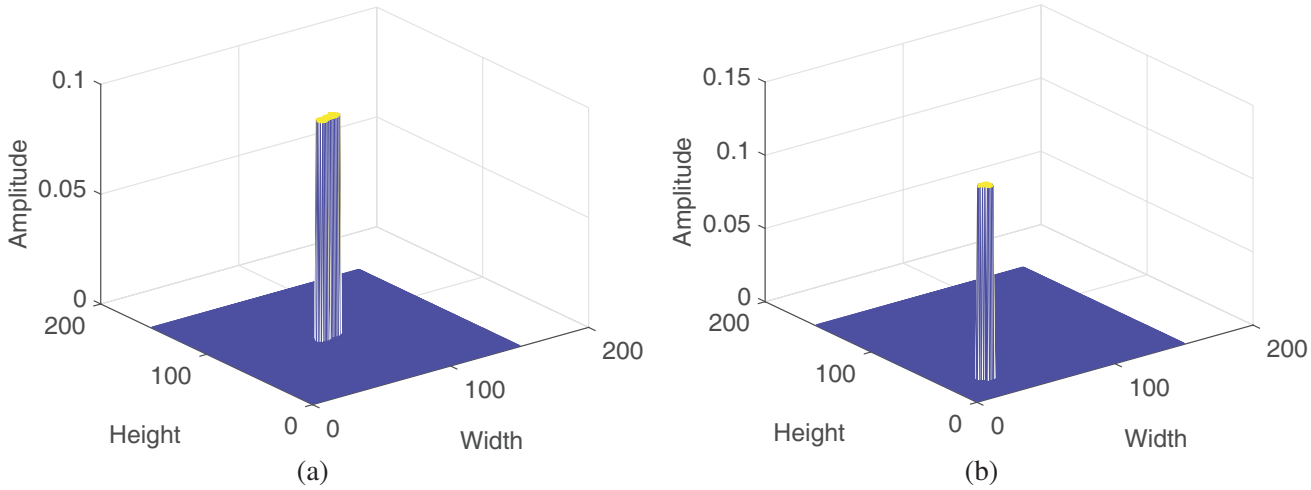

Figure 3. Values F of superpixels. (a) Fig. 2(a). (b) Fig. 2(b).

even if the detector is not CFAR for the background distribution of the data, it still only picks out right pixel values. Experiments and analysis have shown that CFAR detection technology may suffer from performance deterioration due to the changes in ship imaging quality and the influence of complex and unpredictable surroundings [3].

In order to evaluate the performance of the algorithms in a quantitative way, we consider the

Table 1. Comparison of performance for three methods.

Index	Finsler-metric method	Superpixel-level CFAR	Double-parameter CFAR
Detection rate (DR)	81.62%	88.45%	89.99%
False alarm rate (FAR)	4.77%	69.24%	79.54%

(a) (b)

Figure 4. Ship detection results for SAR images of the sea surface. (a) Fig. 3(a). (b) Fig. 3(b).

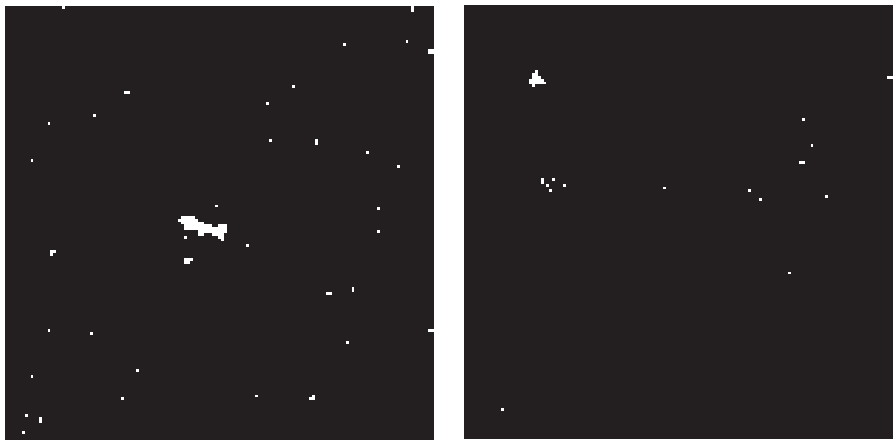

(a) (b)

Figure 5. Double-parameter CFAR detector based on Weibull distribution for ship detection in SAR images. (a) Fig. 1(a). (b) Fig. 1(b).

following evaluation criteria

$$DR = \frac{TP}{TP + FN} \tag{5}$$

$$FAR = \frac{FP}{TP + FP} \tag{6}$$

where DR denotes the detection rate, FAR the false alarm rate, TP the true positive (detected targets), FP the false positive (false alarms), and FN the false negative (missing targets). The performance of the detection methods is demonstrated on Gaofen-3 data [12]. Gaofen-3 is the first civilian C-band polarimetric SAR imaging satellite of China National Space Administration (CNSA), Beijing, China. During the experiment, 5000 SAR images are used to evaluate the performance of detection algorithms. The experimental parameters are set as follows: the guard-band of 15×15 pixels, the background-band of 25×25 pixels, and the constant false alarm rate 10^{-7}. It is shown in Table 1 that the Finsler-metric model has a better false alarm rate, which demonstrates its capability to model the target and clutter.

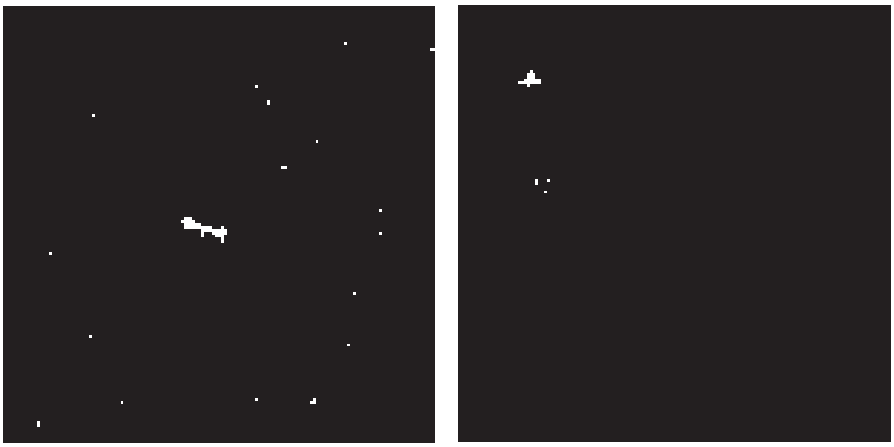

(a) (b)

Figure 6. Superpixel-level CFAR detector based on Weibull distribution for ship detection in SAR images [11]. (a) Fig. 1(a). (b) Fig. 1(b).

4. CONCLUSIONS

In this letter, the structure being focused on is the Finsler geometry. The study has taken on a new look. The ideas and methods of metric spaces and related topics of Finsler geometry not only are closely related to mathematics and physics, but also have more and more applications to information science. It is the aim of this letter to put forward a feasible way for applying Finsler geometric theory in ship detection of SAR images. It provides a feasible framework for further in-depth investigation of Finsler information geometry theory and application.

ACKNOWLEDGMENT

This work was supported by the Open Grant of State Key Laboratory of Complex Electromagnetic Environment Effects on Electronics and Information Systems (CEMEE) under Grant [CEMEE2018Z0203B]; the Zhejiang Province Science and Technology Plan Project under Grant [LGG18F010009].

REFERENCES

1. Wang, X., G. Li, X. Zhang, and Y. He, "Ship detection in SAR images via local contrast of fisher vectors," *IEEE Trans. Geosci. Remote Sens.*, Vol. 58, No. 9, 6467–6479, 2020.
2. Wang, X., G. Li, X. Zhang, and Y. He, "A fast CFAR algorithm based on density-censoring operation for ship detection in SAR images," *IEEE Signal Process. Lett.*, Vol. 28, 1085–1089, 2021.
3. Ai, J., Y. Mao, Q. Luo, M. Xing, K. Jiang, L. Jia, and X. Yang, "Robust CFAR ship detector based on bilateral-trimmed-statistics of complex ocean scenes in SAR imagery: A closed-form solution," *IEEE Trans. Aerosp. Electron. Syst.*, Vol. 57, No. 3, 1872–1890, 2021.
4. Yang, R., G. Wang, Z. Pan, H. Lu, H. Zhang, and X. Jia, "A novel false alarm suppression method for CNN-based SAR ship detector," *IEEE Geosci. Remote Sens. Lett.*, Vol. 18, No. 8, 1401–1405, 2021.
5. Li, X., W. Huang, K. D. Peters, and D. Power, "Assessment of synthetic aperture radar image preprocessing methods for iceberg and ship recognition with convolutional neural networks," *Proc. IEEE Radar Conf.*, 1–5, 2019.
6. Amari, S., *Information Geometry and Its Application*, Springer, Tokyo, 2016.
7. Shen, Y. and Z. Shen, *Introduction to Modern Finsler Geometry*, Science Press, Beijing, 2013.

8. Forbes, C., M. Evans, N. Hastings, and B. Peacock, *Statistical Distributions*, John Wiley & Sons, New York, 2010.
9. Wang, X., C. Chen, Z. Pan, and Z. Pan, "Superpixel-based LCM detector for faint ships hidden in strong noise background SAR imagery," *IEEE Geosci. Remote Sens. Lett.*, Vol. 16, No. 3, 417–421, 2019.
10. Khambampati, A. K., D. Liu, S. K. Konki, and K. Y. Kim, "An automatic detection of the ROI using Otsu thresholding in nonlinear difference EIT imaging," *IEEE Sensors J.*, Vol. 18, No. 12, 5133–5142, 2018.
11. Pappas, O., A. Achim, and D. Bull, "Superpixel-level CFAR detectors for ship detection in SAR imagery," *IEEE Geosci. Remote Sens. Lett.*, Vol. 15, No. 9, 1397–1401, 2018.
12. Xian, S., Z. Wang, Y. Sun, W. Diao, Y. Zhang, and K. Fu, "AIR-SARShip-1.0: High-resolution SAR ship detection dataset," *J. Radars*, Vol. 8, No. 6, 852–862, 2019.